ROCKY MOUNTAIN
JOURNAL OF MATHEMATICS
Volume 46, Number 6, 2016

SINGULAR LINKS AND YANG-BAXTER STATE MODELS

CARMEN CAPRAU, TSUTOMU OKANO
AND DANNY ORTON

ABSTRACT. We employ a solution of the Yang-Baxter equation to construct invariants for knot-like objects. Specifically, we consider a Yang-Baxter state model for the sl(n) polynomial of classical links and extend it to oriented singular links and balanced oriented 4-valent knotted graphs with rigid vertices. We also define a representation of the singular braid monoid into a matrix algebra and seek conditions for further extending the invariant to contain topological knotted graphs. In addition, we show that the resulting Yang-Baxter-type invariant for singular links yields a version of the Murakami-Ohtsuki-Yamada state model for the sl(n) polynomial for classical links.

1. Introduction. The Yang-Baxter equation (YBE) was first introduced in the field of statistical mechanics. It takes its name from the independent work of C.N. Yang in 1968 and R.J. Baxter in 1971. It depends on the idea that, in some scattering situations, particles may preserve their momentum at the cost of changing their quantum internal states. One form of the YBE states that a matrix R, acting on two of the three objects, satisfies

$$(R \otimes I)(I \otimes R)(R \otimes I) = (I \otimes R)(R \otimes I)(I \otimes R),$$

in which case R is called a solution of the YBE. This equation arises when working with braid groups (in which case, R corresponds to swapping two braid strands) and when discussing invariants for knots and links. A relationship between the YBE and polynomial invariants of links was implicitly revealed by Jones in his seminal paper **[2]**, where he introduced a one-variable polynomial of links via a study

2010 AMS *Mathematics subject classification.* Primary 57M15, 57M27.

Keywords and phrases. Graphs, invariants for knots and links, singular braids and links, sl(n) polynomial, Yang-Baxter equation.

This research was supported by NSF grant No. DMS-1156273.

Received by the editors on June 15, 2014, and in revised form on January 18, 2015.

DOI:10.1216/RMJ-2016-46-6-1867

of finite-dimensional von Neumann algebras. The Jones polynomial was almost immediately generalized to a two-variable polynomial for oriented links, see [**1, 9**], the so-called HOMFLY-PT polynomial, which can be defined via a Conway-type skein relation. Using an analogous geometric procedure, Kauffman introduced a two-variable polynomial invariant of regular isotopy for nonoriented knots and links, see [**3, 5**].

Jones showed that the HOMFLY-PT polynomial can be constructed using explicit matrix representations of Hecke algebras, introduced in the quantum scattering method and related it to the YBE. Using Yang-Baxter operators and so-called *enhanced Yang-Baxter operators* (EYB-operators) Turaev [**10**] associated an isotopy invariant of links with each EYB-operator and showed that, for some special EYB-operators, the corresponding invariants are equivalent to the HOMFLY-PT polynomial and the two-variable Kauffman polynomial.

In his book [**6**], Kauffman provides Yang-Baxter state models for certain polynomial invariants for links. These state models use solutions of the YBE.

In recent years, there has been great interest in the study of knot-like objects, including singular links, knotted graphs, and virtual knots. A *knotted graph* is an embedding of a graph in three-dimensional space, and a *singular link* is an immersion of a disjoint union of circles into three-dimensional space, which admits only finitely many singularities that are all transverse double points.

The goal of this paper is to extend Kauffman's Yang-Baxter state model for the sl(n) polynomial (which is a one-variable specialization of the HOMFLY-PT polynomial) to oriented singular links and 4-valent knotted graphs. Along the way, we define a representation of the singular braid monoid. Moreover, we arrive at certain skein relations for planar 4-valent graphs, relations which remind us of the Murakami-Ohtsuki-Yamada (MOY) [**8**] state model for the sl(n)-link invariant. These relations assign well-defined polynomials to planar 4-valent graphs using recursive formulas defined entirely in the category of planar graphs.

We remark that there is an EYB-operator, as in [**10**], associated with the regular isotopy polynomial invariant for singular links constructed here. However, in this paper, we focus on Kauffman's combinatorial approach to Yang-Baxter state models.

1.1. Organization of the paper. In Section 2, we recall the Yang-Baxter state model for the regular isotopy version of the $\mathrm{sl}(n)$ polynomial and introduce some notation. In Section 3, we extend this state model to a regular isotopy invariant for singular links (based on a solution of the YBE) and discuss some of its properties. Then, we use the resulting state model to construct in Section 4 a representation of the singular braid monoid into a matrix algebra over the ring $\mathbb{Z}[q, q^{-1}]$. Section 5 is devoted to showing that our polynomial invariant for singular links yields a version of the MOY state model for the $\mathrm{sl}(n)$ polynomial. Finally, in Section 6, we further extend our polynomial invariant so that it contains balanced, oriented, 4-valent knotted graphs with rigid vertices. We also find a numerical invariant of 4-valent topological knotted graphs.

2. A Yang-Baxter model for the $\mathrm{sl}(n)$ polynomial. In this section, we briefly review the Yang-Baxter state model for the $\mathrm{sl}(n)$ polynomial introduced by Kauffman **[6]**. Given a link diagram D, label its edges with *spins* from the equally spaced index set

$$I_n = \{1 - n, 3 - n, \ldots, n - 3, n - 1\},$$

for $n \in \mathbb{Z}$ and $n \geq 2$, as follows: replace each crossing in D by either a *decorated splice*

or by a *flat crossing*

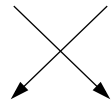
,

and label the resulting diagram σ with spins from the set I_n, so that each loop in σ has constant spin, and so that the spins satisfy the following rules:

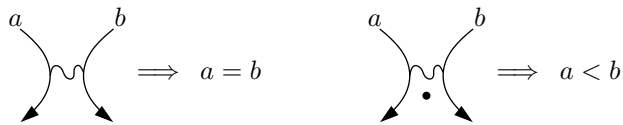

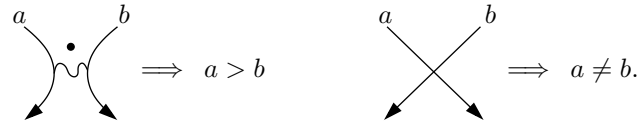

The result is a *state* of D. Note that some of the states will have incompatible labels (spins) and thus are discarded.

Associate to each state σ a polynomial $\langle\sigma\rangle \in \mathbb{Z}[q, q^{-1}]$ given by:

$$\langle\sigma\rangle = q^{\|\sigma\|}, \qquad \|\sigma\| = \sum_l \operatorname{rot}(l) \cdot \operatorname{label}(l), \tag{2.1}$$

where the sum is taken over all components l in σ, $\operatorname{label}(l)$ is the spin assigned to the loop l, and where $\operatorname{rot}(l)$ is the *rotation number* of l given by:

$$\operatorname{rot}\left(\text{  }\right) = 1, \qquad \operatorname{rot}\left(\text{  }\right) = -1.$$

Example 2.1. For state σ_1 below, $\langle\sigma_1\rangle = q^{2a-b}$. On the other hand, the state σ_2 will have incompatible spins for any choice of labels, and thus it is discarded. Equivalently, we set $\langle\sigma_2\rangle = 0$.

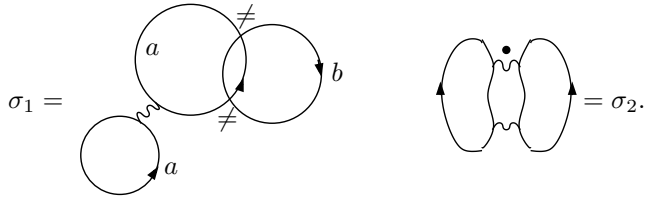

The $\mathrm{sl}(n)$ *polynomial* of the link diagram D is given by:

$$\langle D\rangle = \sum_\sigma a_\sigma \langle\sigma\rangle = \sum_\sigma a_\sigma q^{\|\sigma\|}, \tag{2.2}$$

where the sum is taken over all states σ of D and where a_σ is the product of the weights associated with a state σ according to the skein relations given in Figure 1.

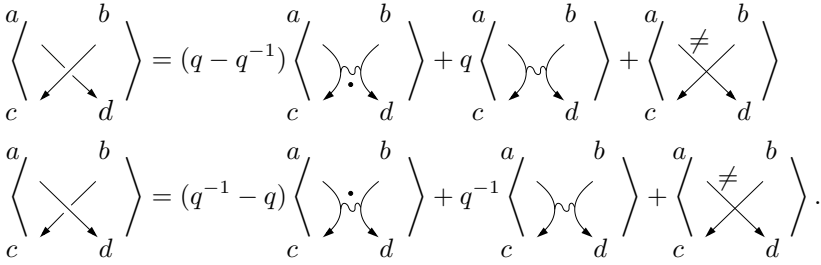

FIGURE 1. Crossings decomposition.

The diagrams on the two sides of the skein relations in Figure 1 represent parts of bigger link diagrams that are similar, except in a small neighborhood where they differ as shown in the given relation.

According to the rules in Figure 1, and due to the requirement that each loop in state σ with $\langle\sigma\rangle \neq 0$ has constant spin, it follows that the evaluation of a crossing is non-zero only when the spins a, b, c and d associated with the four endpoints of the crossing satisfy the conservation law, $a + b = c + d$. In particular, the evaluation of a crossing is non-zero if and only if $a = c$ and $b = d$ or $a = d$ and $b = c$.

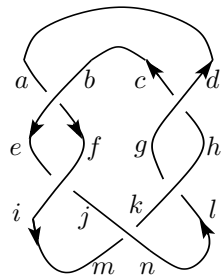

FIGURE 2. A diagram as an abstract tensor diagram.

We can arrive at the sl(n) polynomial $\langle D\rangle$ by interpreting link diagrams as *abstract tensor diagrams*. An oriented link diagram D can be decomposed with respect to a height function into minima (creations), maxima (annihilations) and crossings (interactions), as illustrated in Figure 2, that is, the diagram D is constructed from

interconnected maxima, minima and crossings. We want to associate to them square matrices with entries in $\mathbb{Z}[q, q^{-1}]$.

We associate the symbols R_{cd}^{ab} and $\overline{R}_{cd}^{ab}$ to the positive and negative crossings, respectively:

$R_{cd}^{ab} =$ 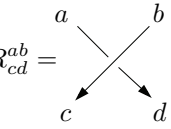

$\overline{R}_{cd}^{ab} =$ 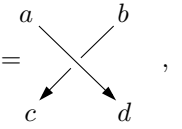

,

where $a, b, c, d \in I_n$. With these conventions, the skein relations in Figure 1 can be rewritten as follows:

$$R_{cd}^{ab} = (q - q^{-1})[a < b]\ \delta_c^a\ \delta_d^b + q[a = b]\ \delta_c^a\ \delta_d^b + [a \neq b]\ \delta_d^a\ \delta_c^b,$$
$$\overline{R}_{cd}^{ab} = (q^{-1} - q)[a > b]\ \delta_c^a\ \delta_d^b + q^{-1}[a = b]\ \delta_c^a\ \delta_d^b + [a \neq b]\ \delta_d^a\ \delta_c^b,$$

where

$[a = b]\delta_c^a\delta_d^b =$ 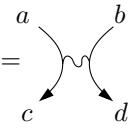

$[a < b]\delta_c^a\delta_d^b =$ 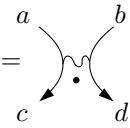

$[a > b]\delta_c^a\delta_d^b =$ 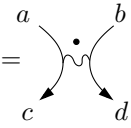

$[a \neq b]\delta_d^a\delta_c^b =$ 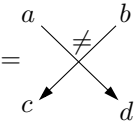

,

and where

$$[P] = \begin{cases} 1 & \text{if P is true,} \\ 0 & \text{if P is false,} \end{cases} \qquad \text{and} \quad \overset{a}{\underset{c}{\frown}} = \delta_c^a = \begin{cases} 1 & \text{if } a = c, \\ 0 & \text{if } a \neq c. \end{cases}$$

We associate the symbols $\overrightarrow{M}^{ab}$, $\overleftarrow{M}^{ab}$ and $\overrightarrow{M}_{ab}$, $\overleftarrow{M}_{ab}$ to oriented minima and maxima, respectively, and we put

$\overrightarrow{M}^{ab} =$ 

$= q^{a/2}\delta^{a,b}$ $\qquad$ $\overleftarrow{M}^{ab} =$ 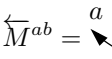

$= q^{-a/2}\delta^{a,b}$

$\overleftarrow{M}_{ab} =$  $= q^{a/2}\delta^{a,b}$ $\qquad$ $\overrightarrow{M}_{ab} =$ 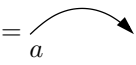 $= q^{-a/2}\delta^{a,b}$,

where

$$\delta^{a,b} = \begin{cases} 1 & a = b, \\ 0 & a \neq b. \end{cases}$$

Therefore, for diagram D in Figure 2, the evaluation $\langle D \rangle$ is given by the following sum of the product of matrix entries:

$$\langle D \rangle = \sum_{a,b,\ldots,n \in I_n} \overleftarrow{M}_{ad}\, \overleftarrow{M}_{bc}\, R^{ab}_{ef}\, R^{ef}_{ij}\, \overrightarrow{M}^{im}\, R^{mj}_{nk}\, \overrightarrow{M}^{nl}\, R^{lk}_{hg}\, R^{hg}_{dc},$$

where the sum is over all possible choices of indices (spins from I_n) in the expression.

It is important to note that the above conventions yield the necessary loop value, namely,

$$[n] = \frac{q^n - q^{-n}}{q - q^{-1}},$$

where $[n]$ is the quantum integer n. On the one hand,

$$\left\langle \text{  } \right\rangle = \sum_{a \in I_n} \left\langle a\text{  } \right\rangle = \sum_{a \in I_n} q^a = [n],$$

and, on the other hand,

$$\sum_{a \in I_n} \left\langle a\text{  } \right\rangle = \sum_{a \in I_n} \left(\sum_{b \in I_n} \overleftarrow{M}_{ab} \overrightarrow{M}^{ab} \right) = \sum_{a \in I_n} q^a.$$

Moreover, the loop value stays the same if the circle is oriented clockwise, since

$$\sum_{a \in I_n} q^a = q^{1-n} + q^{3-n} + \cdots + q^{n-3} + q^{n-1} = \sum_{a \in I_n} q^{-a}.$$

Observe that the creation and annihilation matrices satisfy

$$\sum_{i \in I_n} \overrightarrow{M}^{ai} \overrightarrow{M}_{ib} = \delta^a_b = \sum_{i \in I_n} \overleftarrow{M}_{bi}\, \overleftarrow{M}^{ia},$$

$$\sum_{i \in I_n} \overleftarrow{M}^{ai} \overleftarrow{M}_{ib} = \delta^b_a = \sum_{i \in I_n} \overrightarrow{M}_{bi}\, \overrightarrow{M}^{ia},$$

which correspond, respectively, to the following planar isotopies (canceling pairs of maxima and minima):

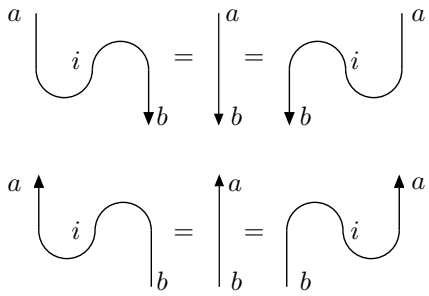

The matrices R and $\overline{R}$ satisfy the *channel unitarity*:

$$\sum_{i,i\in I_n} R_{ij}^{ab}\,\overline{R}_{cd}^{ij} =$$

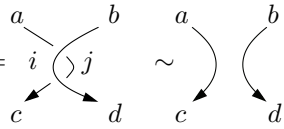

$$= \delta_c^a\,\delta_d^b,$$

and the *cross-channel unitarity*:

$$\sum_{i,j\in I_n} \overline{R}_{jb}^{ia}\,R_{ic}^{jd} =$$

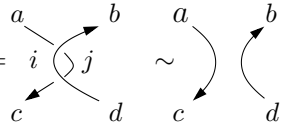

$$= \delta_c^a\,\delta_b^d.$$

Moreover, we have that

$$\sum_{i,j,k\in I} R_{ij}^{ab} R_{kf}^{jc}\,R_{de}^{ik} =$$

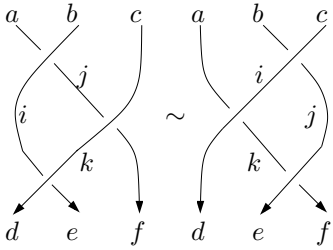

$$= \sum_{i,j,k\in I} R_{ij}^{bc} R_{dk}^{ai}\,R_{ef}^{kj}.$$

The latter relation is the Yang-Baxter equation (YBE):

$$\sum_{i,j,k\in I} R_{ij}^{ab} R_{kf}^{jc}\,R_{de}^{ik} = \sum_{i,j,k\in I} R_{ij}^{bc} R_{dk}^{ai}\,R_{ef}^{kj},$$

that is, the R matrix (as defined above) is a solution of the YBE. Similarly, the matrix $\overline{R}$ is a solution of the YBE. Moreover,

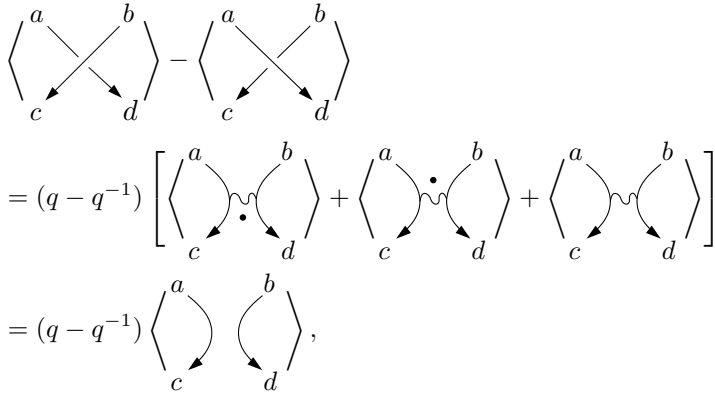

where the last equality holds since the three states have non-zero evaluations if and only if $c = a$ and $d = b$, and since the spins a and b are either $a < b$, $a > b$ or $a = b$.

It follows that the polynomial $\langle D \rangle$ is an invariant of regular isotopy for oriented links. Moreover, the following hold:

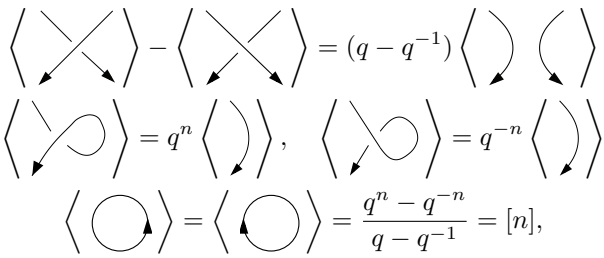

which implies that $\langle D \rangle$ is the regular isotopy version of the sl(n) -link invariant.

3. An invariant for singular links. A *singular link* is an immersion of a disjoint union of circles in $\mathbb{R}^3$ which admits only finitely many singularities that are all transverse double points. A *knotted graph* (also called a *spacial graph*) is an embedding of a graph in $\mathbb{R}^3$. A singular link can be regarded as a 4-valent rigid-vertex embedding of a graph

in $\mathbb{R}^3$. In this paper, we consider only 4-valent knotted graphs, that is, graphs whose vertices have degree 4.

Two singular links are called equivalent if their diagrams differ by a finite sequence of classical Reidemeister moves together with the extended Reidemeister moves $R4$ and $R5$ shown in Figure 3.

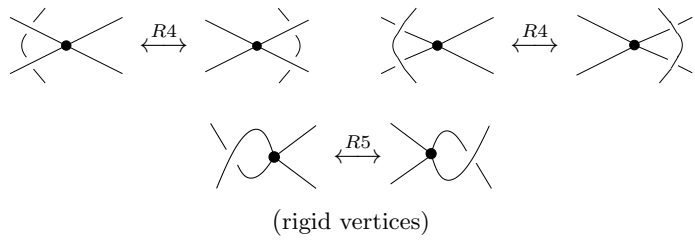

FIGURE 3. The moves $R4$ and $R5$.

Note that the move $R5$ preserves the ordering of the edges meeting at a singular crossing. In graph-theoretical language, this means that we regard a singular crossing as a rigid disk. Each disk has four arcs attached to it, and the cyclic order of these arcs is determined via the rigidity of the disk. A rigid vertex isotopy of the embeddings of such a graph G in three-space consists of affine motions of the disks, together with topological ambient isotopies of the edges of G. As mentioned above, the collection of moves that generate rigid vertex isotopy for diagrams of 4-valent graph embeddings are classical Reidemeister moves coupled with the moves $R4$ and $R5$ depicted above, see [**4**].

On the other hand, two 4-valent knotted graphs are equivalent if their diagrams differ by a finite sequence of classical Reidemeister moves together with the extended Reidemeister moves $R4$ and $R6$. The Reidemeister move of type 6 is depicted in Figure 4. For more details on equivalent knotted graphs we refer the reader to Kauffman's work [**4**].

In this paper, all singular links and knotted graphs are oriented. Our first goal is to extend the Yang-Baxter state model for the $\mathrm{sl}(n)$ link polynomial described in Section 2 to oriented singular links.

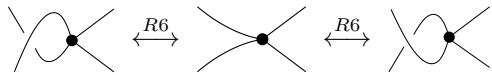

FIGURE 4. The move $R6$.

Given a singular link diagram G, we label its edges with spins from the equally spaced index set $I_n = \{1-n, 3-n, \ldots, n-3, n-1\}$, for $n \in \mathbb{Z}$ and $n \geq 2$, and we decompose the classical crossings according to the skein relations in Figure 1. We need to define a skein relation involving a singular crossing of G. For example, we can impose the following skein relation for some $\alpha, \beta \in \mathbb{Z}[q, q^{-1}]$:

(3.1)
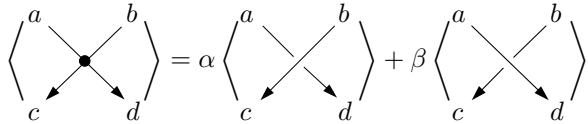

Then, we evaluate the resulting states of G using formula (2.1). Combining everything, we obtain a Laurent polynomial $\langle G \rangle$ associated with a singular link diagram G, given by

$$\langle G \rangle = \sum_{\sigma} b_\sigma \, \langle \sigma \rangle = \sum_{\sigma} b_\sigma \, q^{\|\sigma\|}, \tag{3.2}$$

where the sum is taken over all states σ of G and where b_σ is the product of weights associated with state σ according to the skein relations given in equation (3.1) and Figure 1.

We remind the reader that, given an invariant of regular isotopy for classical links, the invariant can be extended via relation (3.1) to a regular isotopy invariant of singular links. Translating this into our case, we arrive at the next result.

Theorem 3.1. *The Laurent polynomial $\langle G \rangle(q) \in \mathbb{Z}[q, q^{-1}]$ is an invariant of regular isotopy for oriented singular links G, for any $\alpha, \beta \in \mathbb{Z}[q, q^{-1}]$, and satisfies*

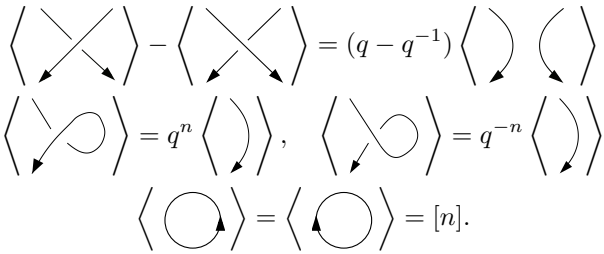

Proof. Since $\langle G \rangle$ is an extension of the Yang-Baxter state model for the sl(n) link invariant, it immediately follows that $\langle G \rangle$ is invariant under the type 2 and type 3 Reidemeister moves, and that it satisfies the above three relations. It is easy to see that $\langle G \rangle$ is invariant under the extended $R4$ move; this follows from equation (3.1) and the fact that $\langle G \rangle$ is invariant under the Reidemeister move of type 3. Below, we show that $\langle G \rangle$ is invariant under the move $R5$:

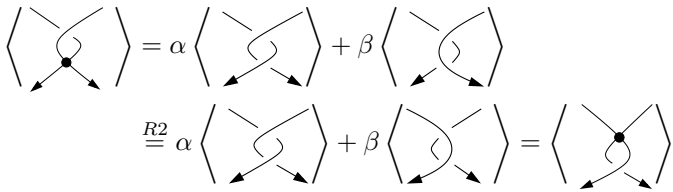

which completes the proof. □

For the remainder of the paper, we work with

$$\alpha = \frac{q}{q - q^{-1}} \quad \text{and} \quad \beta = \frac{-q^{-1}}{q - q^{-1}}$$

in equation (3.1). This results in the singular crossing decomposition displayed in Figure 5.

Note that the evaluation of a singular crossing is non-zero only when the spins a, b, c and d associated with the four edges incident with the singular crossing satisfy $a + b = c + d$. Specifically, the evaluation of a singular crossing is non-zero only when $a = c$ and $b = d$ or $d = a \neq b = c$. It is important to note the difference between the left-hand side of the skein relation in Figure 5 and the last term on the right-hand side of the same skein relation. The latter makes use of

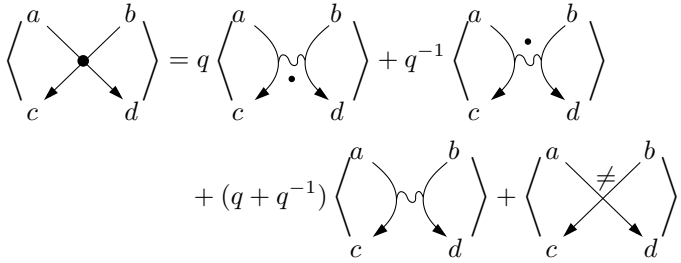

FIGURE 5. Singular crossing decomposition.

spins a, b, c and d such that $d = a \neq b = c$ and is a decorated state of singular crossings.

Denote the $n^2 \times n^2$ square matrix corresponding to a singular crossing by Q. Then, the latter skein relation can be rewritten in terms of the entries of matrix Q as follows:

$$\begin{aligned} Q_{cd}^{ab} = {} & q[a < b]\delta_c^a\delta_d^b + q^{-1}[a > b]\delta_c^a\delta_d^b \\ & + (q + q^{-1})[a = b]\delta_c^a\delta_d^b + [a \neq b]\delta_d^a\delta_c^b, \end{aligned}$$

for all $a, b, c, d \in I_n$. Note that, since $\langle G \rangle$ is invariant under the move $R5$, this implies that $RQ = QR$ and $\overline{R}Q = Q\overline{R}$.

Example 3.2. Using abstract tensor diagrams and matrices R, $\overline{R}$ and Q, the Laurent polynomial $\langle G \rangle$ associated with diagram G depicted in Figure 6 is given by:

$$\langle D \rangle = \sum_{a,b,\ldots,n \in I_n} \overleftarrow{M}_{ad}\overleftarrow{M}_{bc}R_{ef}^{ab}R_{ij}^{ef}\overrightarrow{M}^{im}Q_{nk}^{mj}\overrightarrow{M}^{nl}R_{hg}^{lk}Q_{dc}^{hg}, \tag{3.3}$$

where the sum is over all possible choices of indices (spins from I_n) in equation (3.3).

Proposition 3.3. *For*

$$\alpha = \frac{q}{q - q^{-1}} \quad \textit{and} \quad \beta = \frac{-q^{-1}}{q - q^{-1}},$$

the following skein relations hold:

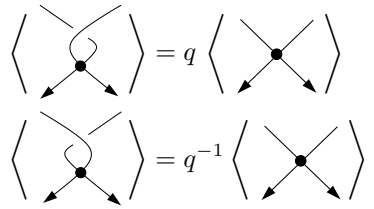

Proof. The first step below makes use of the crossing decomposition from Figure 1 applied to the left side of the first equality, which results in three diagrams. Then, we apply the skein relation depicted in Figure 5 to each of the resulting diagrams.

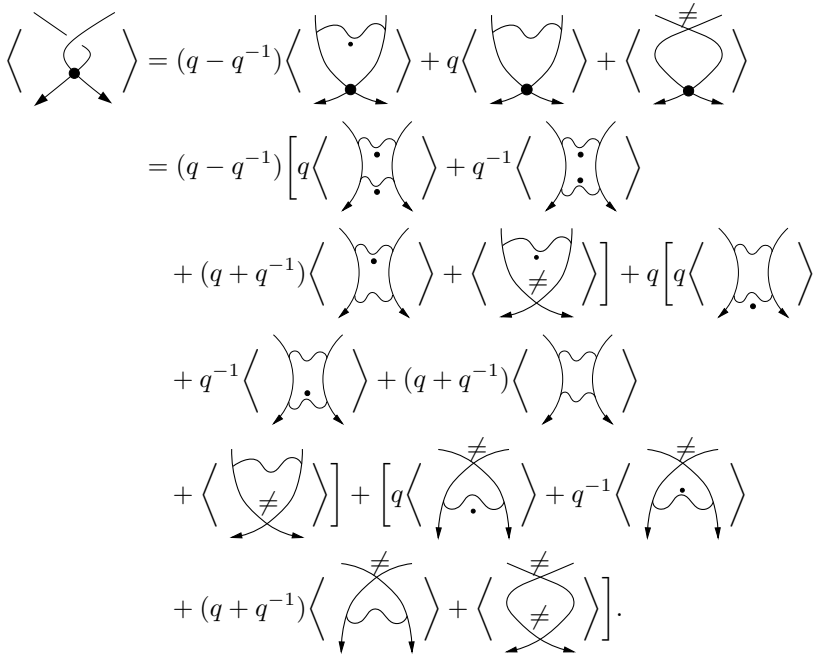

Some of the diagrams above evaluate to 0 due to incompatible labeling

of the strands, specifically,

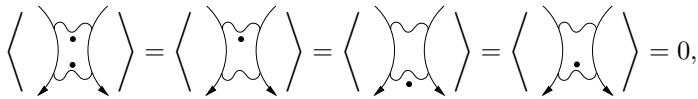

and

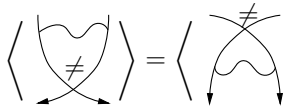

In addition, note that

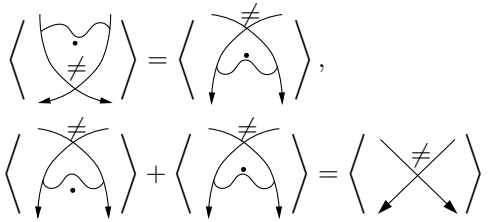

Combining these, we have

(3.4)

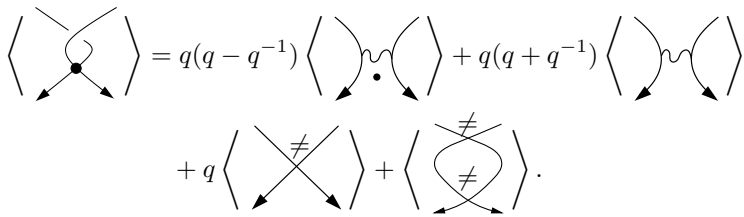

Moreover, since

equation (3.4) is equivalent to

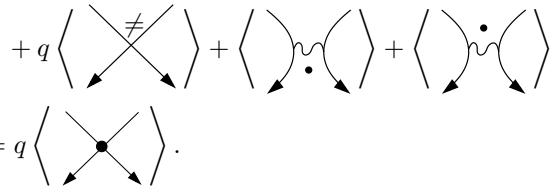

Therefore, the first skein relation holds. The second relation is proved in a similar fashion. □

The *mirror image* of a singular link with diagram G is the singular link whose diagram G^* is obtained from G by replacing each (classical) positive crossing with a negative crossing and vice versa. A singular link is said to be *achiral* if it is ambient isotopic to its mirror image; otherwise, G is called *chiral*.

Proposition 3.4. *Let G be an oriented singular link, and let G^* be its mirror image. Then the polynomial $\langle G^* \rangle$ is obtained from $\langle G \rangle$ by replacing q with q^{-1}, that is,*

$$\langle G^* \rangle(q) = \langle G \rangle(q^{-1}).$$

Proof. Diagram G^* is obtained from G by reversing all classical crossings, which has the effect of interchanging q and q^{-1} in the definition of $\langle \cdot \rangle$. On the other hand, the evaluation of a singular crossing remains the same when q and q^{-1} are interchanged. Therefore, the statement holds. □

Corollary 3.5. *If $\langle G \rangle(q) \neq \langle G \rangle(q^{-1})$, then G is a chiral singular link.*

Proposition 3.6. *Let $G_1 \cup G_2$ be the disjoint union of oriented singular links G_1 and G_2. Then,*

$$\langle G_1 \cup G_2 \rangle = \langle G_1 \rangle \langle G_2 \rangle.$$

Proof. Note that this formula holds when G_1 and G_2 are classical links, that is, when G_1 and G_2 have no singular crossings. Then the statement is verified for singular links using a standard proof by induction on the number of singular crossings, and thus it is omitted. □

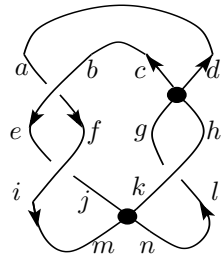

FIGURE 6. An abstract tensor singular link diagram.

A singular link diagram G is a *connected sum*, denoted by $G = G_1 \# G_2$ if it is displayed as two disjoint singular link diagrams G_1 and G_2 connected by parallel embedded arcs, up to planar isotopy, as in Figure 7. The following result holds for classical links, and can be proved for singular links, as well, by induction on the number of singular crossings.

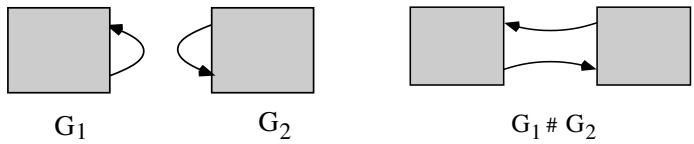

FIGURE 7. A connected sum.

Proposition 3.7. *Let G be an oriented singular link diagram with the property that $G = G_1 \# G_2$, for some oriented singular link diagrams G_1 and G_2. Then the polynomial $\langle G \rangle$ can be computed as follows*:

$$\langle G \rangle = \frac{1}{[n]} \langle G_1 \rangle \langle G_2 \rangle.$$

4. Representations of the singular braid monoid. Let G be a singular link diagram, and consider the polynomial $\langle G \rangle$ defined by equation (3.2), with

$$\alpha = \frac{q}{q - q^{-1}} \quad \text{and} \quad \beta = \frac{-q^{-1}}{q - q^{-1}}.$$

In this section, we show how to use the Yang-Baxter state model for $\langle G \rangle$ to define, for each $n \in \mathbb{Z}$ and $n \geq 2$, a representation of the singular braid monoid into a matrix algebra.

Recall that the $n^2 \times n^2$ matrices R and $\overline{R}$ associated with a positive and a negative crossing, respectively (and satisfying the YBE), and the $n^2 \times n^2$ matrix Q correspond to a singular crossing. These matrices have entries given by:

$$\begin{aligned}
R_{cd}^{ab} &= (q - q^{-1})[a < b]\ \delta_c^a\ \delta_d^b + q[a = b]\ \delta_c^a\ \delta_d^b + [a \neq b]\ \delta_d^a\ \delta_c^b, \\
\overline{R}_{cd}^{ab} &= (q^{-1} - q)[a > b]\ \delta_c^a\ \delta_d^b + q^{-1}[a = b]\ \delta_c^a\ \delta_d^b + [a \neq b]\ \delta_d^a\ \delta_c^b, \\
Q_{cd}^{ab} &= q[a < b]\delta_c^a\delta_d^b + q^{-1}[a > b]\delta_c^a\delta_d^b \\
&\quad + (q + q^{-1})[a = b]\delta_c^a\delta_d^b + [a \neq b]\delta_d^a\delta_c^b,
\end{aligned}$$

for all $a, b, c, d \in I_n$, that is, the matrices $R = (R_{cd}^{ab})$ and $\overline{R} = (\overline{R}_{cd}^{ab})$ are as follows:

$$R_{cd}^{ab} = \begin{cases} q - q^{-1} & \text{if } c = a < b = d, \\ q & \text{if } c = a = b = d, \\ 1 & \text{if } d = a \neq b = c, \\ 0 & \text{otherwise.} \end{cases}$$

$$\overline{R}_{cd}^{ab} = \begin{cases} q^{-1} - q & \text{if } c = a > b = d, \\ q^{-1} & \text{if } c = a = b = d, \\ 1 & \text{if } d = a \neq b = c, \\ 0 & \text{otherwise.} \end{cases}$$

In addition, the matrix $Q = (Q_{cd}^{ab})$ is given by:

$$Q_{cd}^{ab} = \begin{cases} q + q^{-1} & \text{if } c = a = b = d, \\ q & \text{if } c = a < b = d, \\ q^{-1} & \text{if } c = a > b = d, \\ 1 & \text{if } d = a \neq b = c, \\ 0 & \text{otherwise.} \end{cases}$$

For $n = 2$, the index set is $I_2 = \{-1, 1\}$, given the following matrices:

$$R_2 = \begin{bmatrix} q & 0 & 0 & 0 \\ 0 & q - q^{-1} & 1 & 0 \\ 0 & 1 & 0 & 0 \\ 0 & 0 & 0 & q \end{bmatrix}, \qquad \overline{R}_2 = \begin{bmatrix} q^{-1} & 0 & 0 & 0 \\ 0 & 0 & 1 & 0 \\ 0 & 1 & q^{-1} - q & 0 \\ 0 & 0 & 0 & q^{-1} \end{bmatrix},$$

$$Q_2 = \begin{bmatrix} q + q^{-1} & 0 & 0 & 0 \\ 0 & q & 1 & 0 \\ 0 & 1 & q^{-1} & 0 \\ 0 & 0 & 0 & q + q^{-1} \end{bmatrix}.$$

For $n = 3$, the index set becomes $I_3 = \{-2, 0, 2\}$, and the corresponding matrices R, $\overline{R}$ and Q are:

$$R_3 = \begin{bmatrix} q & 0 & 0 & 0 & 0 & 0 & 0 & 0 & 0 \\ 0 & q - q^{-1} & 0 & 1 & 0 & 0 & 0 & 0 & 0 \\ 0 & 0 & q - q^{-1} & 0 & 0 & 0 & 1 & 0 & 0 \\ 0 & 1 & 0 & 0 & 0 & 0 & 0 & 0 & 0 \\ 0 & 0 & 0 & 0 & q & 0 & 0 & 0 & 0 \\ 0 & 0 & 0 & 0 & 0 & q - q^{-1} & 0 & 1 & 0 \\ 0 & 0 & 1 & 0 & 0 & 0 & 0 & 0 & 0 \\ 0 & 0 & 0 & 0 & 0 & 1 & 0 & 0 & 0 \\ 0 & 0 & 0 & 0 & 0 & 0 & 0 & 0 & q \end{bmatrix}$$

$$\overline{R}_3 = \begin{bmatrix} q^{-1} & 0 & 0 & 0 & 0 & 0 & 0 & 0 & 0 \\ 0 & 0 & 0 & 1 & 0 & 0 & 0 & 0 & 0 \\ 0 & 0 & 0 & 0 & 0 & 0 & 1 & 0 & 0 \\ 0 & 1 & 0 & q^{-1} - q & 0 & 0 & 0 & 0 & 0 \\ 0 & 0 & 0 & 0 & q^{-1} & 0 & 0 & 0 & 0 \\ 0 & 0 & 0 & 0 & 0 & 0 & 0 & 1 & 0 \\ 0 & 0 & 1 & 0 & 0 & 0 & q^{-1} - q & 0 & 0 \\ 0 & 0 & 0 & 0 & 0 & 1 & 0 & q^{-1} - q & 0 \\ 0 & 0 & 0 & 0 & 0 & 0 & 0 & 0 & q^{-1} \end{bmatrix}$$

$$Q_3 = \begin{bmatrix} q+q^{-1} & 0 & 0 & 0 & 0 & 0 & 0 & 0 & 0 \\ 0 & q & 0 & 1 & 0 & 0 & 0 & 0 & 0 \\ 0 & 0 & q & 0 & 0 & 0 & 1 & 0 & 0 \\ 0 & 1 & 0 & q^{-1} & 0 & 0 & 0 & 0 & 0 \\ 0 & 0 & 0 & 0 & q+q^{-1} & 0 & 0 & 0 & 0 \\ 0 & 0 & 0 & 0 & 0 & q & 0 & 1 & 0 \\ 0 & 0 & 1 & 0 & 0 & 0 & q^{-1} & 0 & 0 \\ 0 & 0 & 0 & 0 & 0 & 1 & 0 & q^{-1} & 0 \\ 0 & 0 & 0 & 0 & 0 & 0 & 0 & 0 & q+q^{-1} \end{bmatrix}.$$

It can be shown that, for any fixed $n \in \mathbb{Z}$ and $n \geq 2$,

$$R_n Q_n = Q_n R_n = q \cdot Q_n \quad \text{and} \quad \overline{R}_n Q_n = Q_n \overline{R}_n = q^{-1} \cdot Q_n,$$

which mimic the properties of the polynomial $\langle G \rangle$ discussed in Section 3.

The *singular braid monoid* on k strands, denoted by SB_k, is a monoid with generators σ_i, σ_i^{-1} and τ_i, where $1 \leq i \leq k-1$,

$\sigma_i =$ 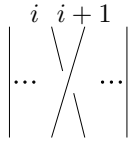

$\sigma_i^{-1} =$ 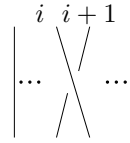

$\tau_i =$ 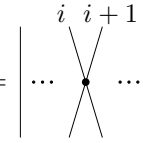

and relations:

(i) $g_i h_j = h_j g_i$, where $|i-j| > 1$ and $g_i, h_i \in \{\sigma_i, \sigma_i^{-1}, \tau_i\}$.
(ii) $\sigma_i^{-1}\sigma_i = 1_n = \sigma_i \sigma_i^{-1}$ $(R2)$.
(iii) $\sigma_i\sigma_j\sigma_i = \sigma_j\sigma_i\sigma_j$, for $|i-j| = 1$ $(R3)$.
(iv) $\tau_i\sigma_j\sigma_i = \sigma_j\sigma_i\tau_j$, for $|i-j| = 1$ $(R4)$.
(v) $\sigma_i\tau_i = \tau_i\sigma_i$ $(R5)$.

Below, we depict the last two relations corresponding to the extended Reidemeister moves of type 4 and type 5:

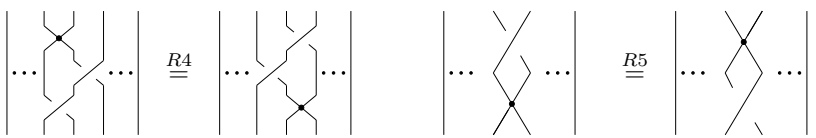

We orient the singular braids so that all strands are oriented downward. Next, we employ the matrices R_n, $\overline{R}_n$ and Q_n to define, for every $n \in \mathbb{N}$ and $n \geq 2$, a homomorphism ρ_n from SB_k into a matrix algebra over $\mathbb{Z}[q, q^{-1}]$, given by:

$$\sigma_1 \longmapsto R_n \otimes I \otimes \cdots \otimes I \qquad \sigma_1^{-1} \longmapsto \overline{R}_n \otimes I \otimes \cdots \otimes I$$

$$\sigma_2 \longmapsto I \otimes R_n \otimes \cdots \otimes I \qquad \sigma_2^{-1} \longmapsto I \otimes \overline{R}_n \otimes \cdots \otimes I$$

$$\cdots$$

$$\sigma_{k-1} \longmapsto I \otimes I \otimes \cdots \otimes R_n \qquad \sigma_{k-1}^{-1} \longmapsto I \otimes I \otimes I \cdots \otimes \overline{R}_n$$

$$\tau_1 \longmapsto Q_n \otimes I \otimes \cdots \otimes I$$

$$\tau_2 \longmapsto I \otimes Q_n \otimes \cdots \otimes I$$

$$\cdots$$

$$\tau_{k-1} \longmapsto I \otimes I \otimes \cdots \otimes Q_n,$$

Here, $\otimes$ is the Kronecker δ tensor product of matrices. Recall that, if A is an $m \times n$ matrix and B is a $p \times q$ matrix, then their Kronecker product $A \otimes B$ is the $mp \times nq$ block matrix:

$$A \otimes B = \begin{bmatrix} a_{11}B & \cdots & a_{1n}B \\ \vdots & \ddots & \vdots \\ a_{m1}B & \cdots & a_{mn}B \end{bmatrix}.$$

Note that, for a k-stranded singular braid β, the associated square matrix $\rho_n(\beta)$ with entries in $\mathbb{Z}[q, q^{-1}]$ has size $n^k \times n^k$. Since the polynomial $\langle G \rangle$ is a regular isotopy invariant for singular links, it implies that the mapping ρ_n preserves the last four singular braid monoid relations. A close look also reveals that, for $|i - j| > 1$, $\rho_n(g_i h_j) = \rho_n(h_j g_i)$, where $g_i, h_i \in \{\sigma_i, \sigma_i^{-1}, \tau_i\}$. This equality holds since the resulting matrices (on both sides of the equality), written as a Kronecker δ tensor product of matrices, will contain the same matrices ($R_n, \overline{R}_n$ or Q_n) on the ith and jth components, respectively, and the $n \times n$ identity matrix on the other components of the tensor product. Therefore, the next statement holds.

Theorem 4.1. *For every $n \in \mathbb{Z}$ and $n \geq 2$, the mapping ρ_n is a representation of the singular braid monoid SB_k into a matrix algebra over $\mathbb{Z}[q, q^{-1}]$.*

5. Another look at sl(n) **invariants.** In this section, we show that the polynomial invariant for singular links constructed in Section 3 can be used to obtain a version of the Murakami-Ohtsuki-Yamada (MOY) state model for the sl(n) polynomial (for details on this state model, we refer the reader to **[8]**). In other words, by extending the Yang-Baxter state model for the sl(n)-link invariant to singular links, we obtain a state model for the sl(n) polynomial, defined via a graphical calculus of planar 4-valent graphs.

We begin with a handy statement, which will be used to derive a set of skein relations involving only planar graphs.

Proposition 5.1. *The following skein relations hold*:

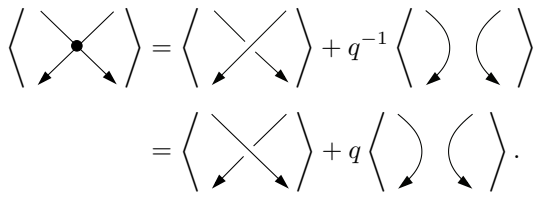

Proof. The statement follows from the skein relations in Figures 1 and 5, as is shown below.

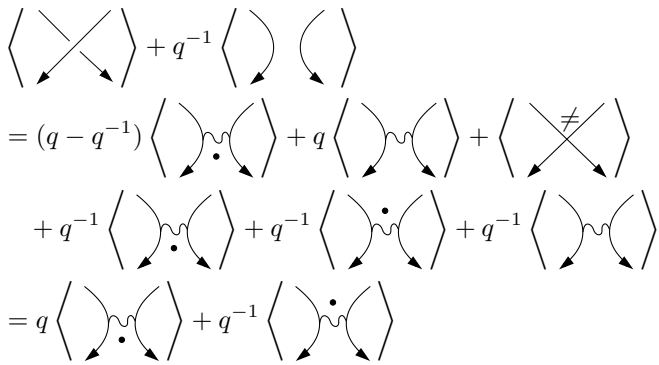

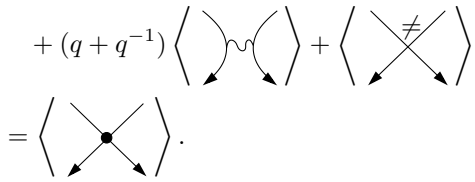

Equation (5.2) can be verified similarly, or by using equation (5.1) together with the exchange skein relation defining the sl(n)-link invariant, as below.

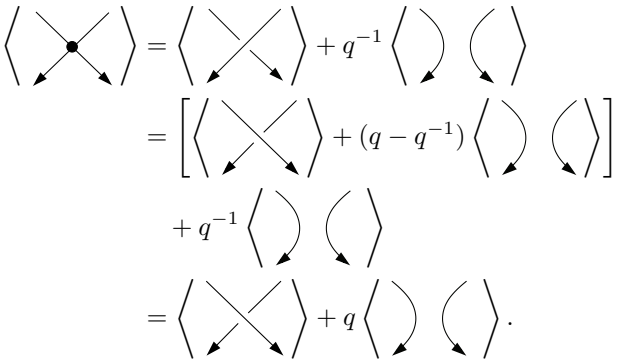

□

Proposition 5.2. *The following graph skein relations hold*:

(5.3)

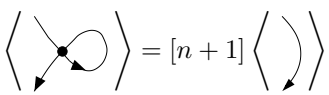

(5.4)

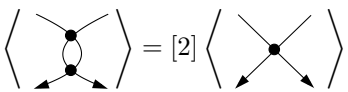

(5.5)

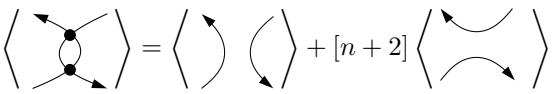

(5.6)

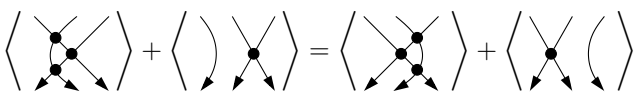

(5.7)

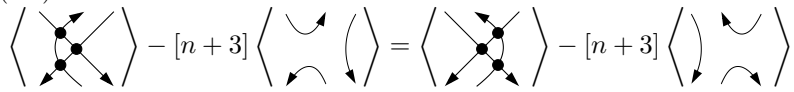

Proof. We will make use of the skein relations in Proposition 5.1. We begin with the first skein relation:

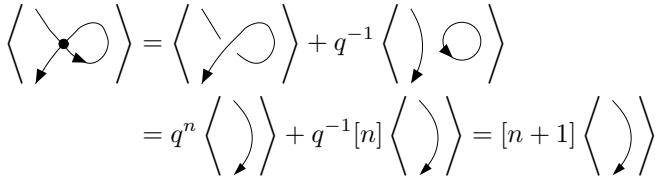

The skein relation in equation (5.4) is verified as follows:

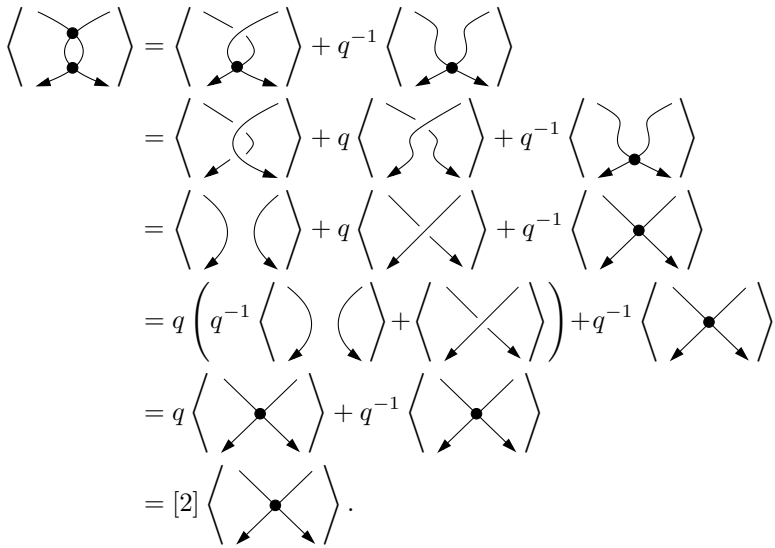

Now, we consider the third skein relation in equation (5.5):

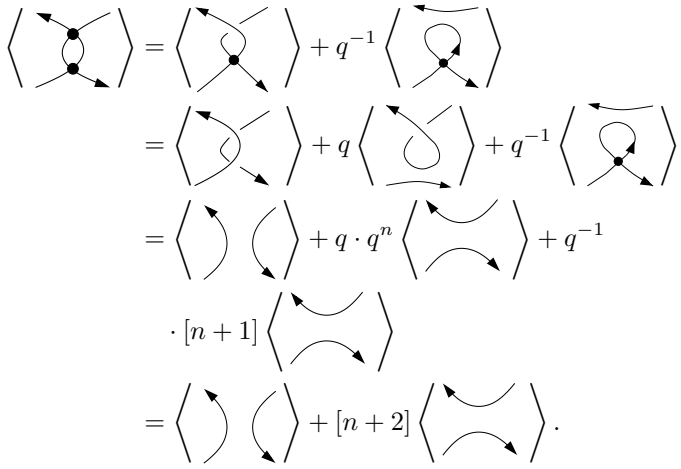

In the latter computations, we used equation (5.3), the invariance of the polynomial under the second Reidemeister move, and the behavior of the polynomial under the first Reidemeister move.

Next, we must show the skein relations in equations (5.6) and (5.7). In order to do this, we first show that the following identities hold:

(5.8)

The first identity in equation (5.8) is verified as shown below; the second identity is verified in a similar manner, and thus it is omitted.

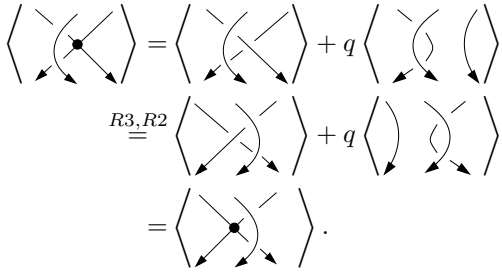

Then, we have:

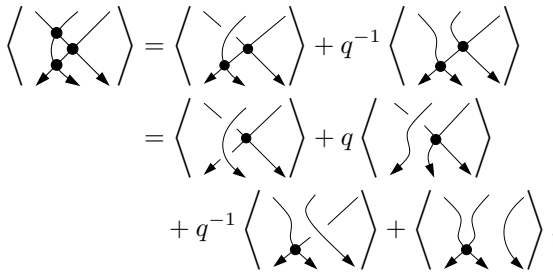

and

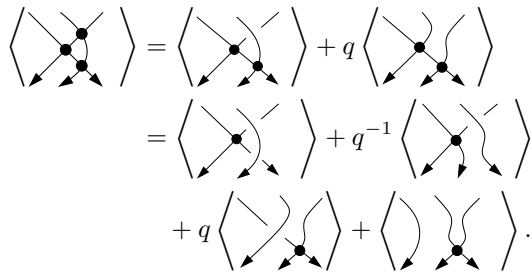

After applying planar isotopies to some of the diagrams above, the skein relation given in equation (5.6) follows.

Finally, we verify the skein relation depicted in equation (5.7).

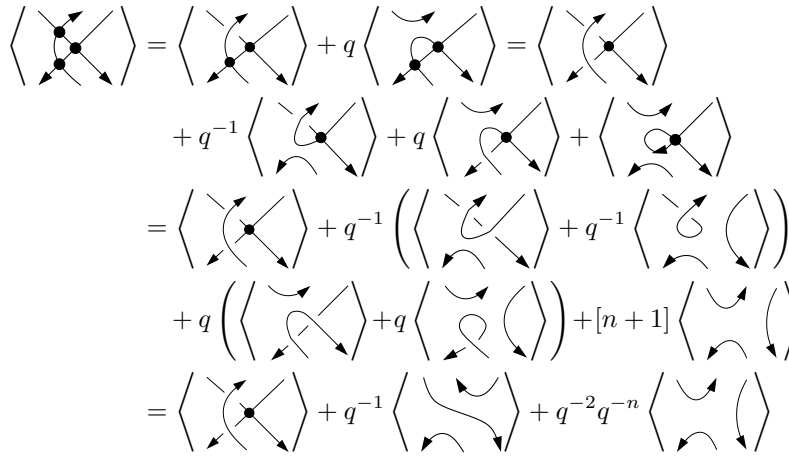

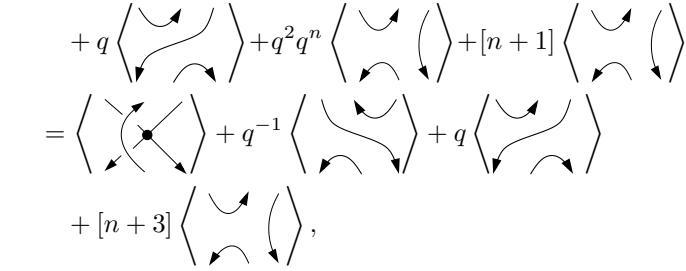

where we used that $q^{-n-2} + q^{n+2} + [n+1] = [n+3]$. Similar computations reveal that

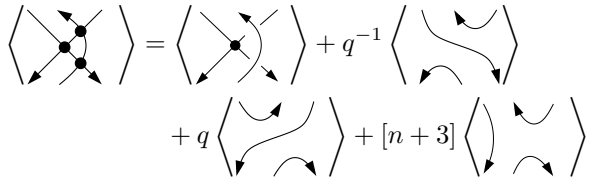

Employing the second identity in equation (5.8), we see that the desired skein relation in equation (5.7) holds. □

Remark 5.3. The graph skein relations given in Proposition 5.2 are consistent and sufficient to uniquely assign a Laurent polynomial in $\mathbb{Z}[q, q^{-1}]$ to any 4-valent planar graph with crossing-type oriented vertices; compare with **[7]**.

Given a link diagram D (or singular link diagram G) we can write each classical crossing in D (or in G) as follows:

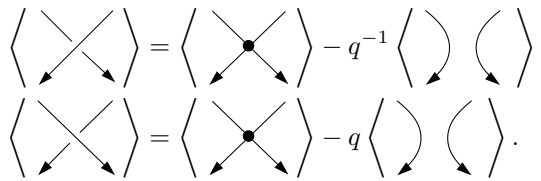

This process results in writing $\langle D \rangle$ (or $\langle G \rangle$) as a $\mathbb{Z}[q, q^{-1}]$-linear combination of evaluations of planar 4-valent graphs with crossing-type oriented vertices. Then, we evaluate the resulting planar graphs using the graph skein relations in Proposition 5.2 and recover the regular isotopy version of the sl(n) polynomial (or our polynomial invariant for

singular links constructed in Section 3). Therefore, this approach provides another method for computing the sl(n) polynomial for oriented knots and links and its extension to singular links.

Remark 5.4. The graphical calculus provided in Proposition 5.2 is a version of the MOY state model for the sl(n) polynomial given in **[8]**, where the wide edges labeled 2 are contracted to result in our 4-valent crossing-type oriented vertices.

6. Balanced oriented knotted graphs. We would like to see whether we can extend our polynomial invariant for singular links constructed in Section 3 (and based on a solution of the YBE) to an invariant that includes oriented knotted graphs. Specifically, the following question arises. Can the polynomial $\langle G \rangle \in \mathbb{Z}[q, q^{-1}]$ be extended such that we obtain an invariant under all versions of the type 6 Reidemeister move shown below?

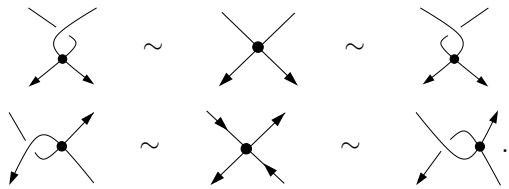

Therefore, we need to consider balanced oriented knotted graphs containing not only crossing-type oriented vertices, but also the alternating oriented vertices:

We will denote the extended polynomial by $[\,\cdot\,]$, and we impose the skein relation

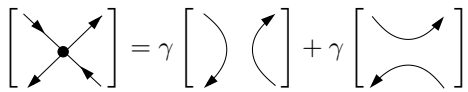

for some $\gamma \in \mathbb{Z}[q, q^{-1}]$. We also impose that $[\,\cdot\,]$ satisfies the skein relations given in Figures 1 and 5, that is, if G is a singular link diagram, then $[G] := \langle G \rangle$.

Theorem 6.1. *The polynomial* $[\,\cdot\,]$ *is a regular isotopy invariant for balanced oriented knotted graphs with rigid vertices.*

Proof. Because $[\,\cdot\,]$ satisfies the skein relations given in Figures 1 and 5, it is invariant under the moves $R2$ and $R3$, as well as under the moves $R4$ and $R5$ for crossing-type oriented vertices. It remains to show that $[\,\cdot\,]$ is invariant under the moves $R4$ and $R5$ for alternating oriented vertices. We first look at the move $R4$:

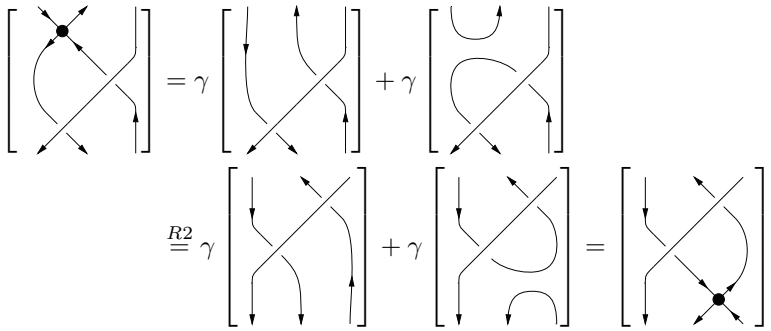

Now, we show the invariance of $[\,\cdot\,]$ under the move $R5$ for alternating oriented vertices:

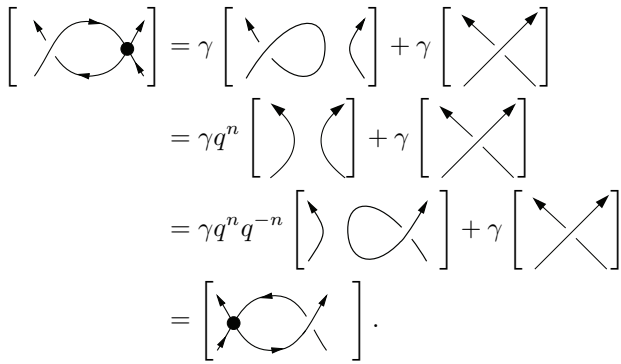

This completes the proof. □

Theorem 6.1 says that $[\,\cdot\,]$ is invariant under the moves $R2$, $R3$, $R4$ and $R5$, but not under the move $R6$. Can we do better than this? Can we obtain an invariant for balanced oriented *topological* knotted

graphs? By Proposition 3.3, we have

Therefore, we would like the following to hold, as well:

(6.1)

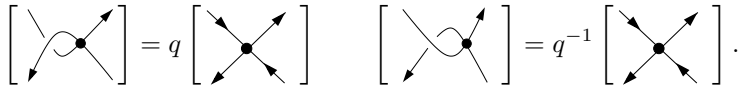

Once the identities in equation (6.1) are satisfied, we can do the following. Given G, a balanced oriented knotted graph diagram, let $\epsilon(G)$ be the writhe of G given by the summation of the signs of all crossings in G, where

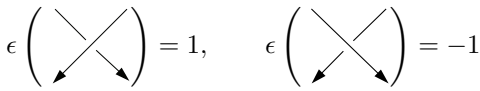

and let

$$P(G) = q^{-\epsilon(G)}[G].$$

We see that, if the identities in equation (6.1) hold, then $P(G)$ is a regular isotopy invariant for balanced oriented topological knotted graphs. Using the skein relations in Proposition 5.1, we have

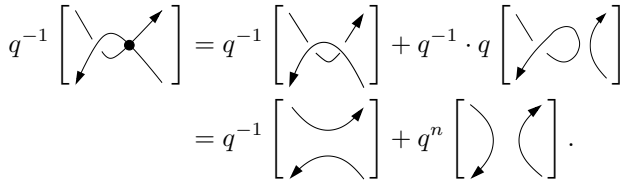

Similarly,

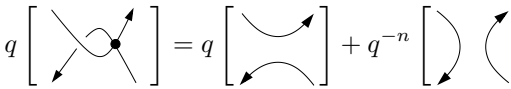

Imposing the equalities in equation (6.1), we see that we need

$$q^n = q^{-n} = \gamma \quad \text{and} \quad q = q^{-1} = \gamma,$$

or equivalently, $q = \pm 1$. We obtain that $P(G)_{|q=\pm 1}$ is an ambient isotopy numerical invariant for balanced oriented topological knotted

graphs. However, if $q = \pm 1$, the skein relation defining the regular isotopy version of the sl(n) link polynomial and its extension to knotted graphs implies that

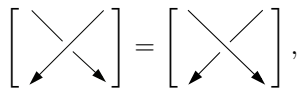

and, therefore, this numerical invariant does not distinguish between different embeddings of a graph, which is rather disappointing.

7. Concluding remarks. In this paper, we employed a solution of the Yang-Baxter equation to construct, for each integer $n \geq 2$, a polynomial invariant $\langle \cdot \rangle$ of regular isotopy for singular links. Then, we studied some properties of the resulting polynomials. These polynomials can also be defined via the representations ρ_n introduced in Section 4. For each fixed integer $n \geq 2$, we further extended the polynomial $\langle \cdot \rangle$ to allow not only crossing-type oriented vertices but also alternating oriented vertices. We showed that the resulting Laurent polynomial $[\cdot]$ is an invariant of rigid-vertex regular isotopy for balanced oriented knotted graphs. In addition, in Section 5, we showed an interesting connection between our polynomial $\langle \cdot \rangle$ for singular links and the MOY state model for the sl(n) polynomial for classical knots and links.

Acknowledgments. This research was partially completed during the 2013 Fresno State Mathematics REU Program. The authors would like to thank the referee for her/his careful reading of the paper and valuable comments and suggestions.

REFERENCES

1. P. Freyd, D. Yetter, J. Hoste, W.B.R. Lickorish, K. Millett and A. Ocneanu, *A new polynomial invariant of knots and links*, Bull. Amer. Math. Soc. **12** (1985), 239–246.

2. V.F.R. Jones, *A polynomial invariant for knots via von Neumann algebras*. Bull. Amer. Math. Soc. **12** (1985), 103–111.

3. L.H. Kauffman, *New invariants in the theory of knots*, Amer. Math. Month. **95** (1988), 195–242.

4. ———, *Invariants of graphs in three-space*, Trans. Amer. Math. Soc. **311** (1989), 697–710.

5. L.H. Kauffman, *An invariant of regular isotopy*, Trans. Amer. Math. Soc. **318** (1990), 417–471.

6. ———, *Knots and physics*, Third edition, in *Series on knots and everything* **1**, World Scientific Publishing, 2001.

7. L.H. Kauffman and P. Vogel, *Link polynomials and a graphical calculus*, J. Knot Theor. Ramifications **1** (1992), 59–104.

8. H. Murakami, T. Ohtsuki and S. Yamada, *Homfly polynomial via an invariant of colored plane graphs*, Enseign. Math. **44** (1998), 325–360.

9. J.H. Przytycki and P. Traczyk, *Invariants of links of Conway type*, Kobe J. Math. **2** (1987), 115–139.

10. V.G. Turaev, *The Yang-Baxter equation and invariants of links*, Invent. Math. **92** (1988), 527–553.

Department of Mathematics, California State University, 5245 North Backer Avenue M/S 108, Fresno, CA 93740
Email address: **ccaprau@csufresno.edu**

Department of Mathematical Sciences, Carnegie Mellon University, Wean Hall 6113, Pittsburgh, PA 15213
Email address: **okano2@illinois.edu**

Department of Mathematics, California State University, 800 N. State College Blvd., Fullerton, CA 92831
Email address: **ortondanny@gmail.com**